

# Navigating Galileo at Jupiter Arrival

R. J. Haw,\* P. G. Antreasian,† T. P. McElrath,† E. J. Graat,† and F. T. Nicholson‡

*Jet Propulsion Laboratory, California Institute of Technology, Pasadena, California 91109*

**Analysis of Doppler tracking data from the Galileo spacecraft contributed to a successful encounter with Jupiter and one of its moons, Io, as well as to the successful delivery of the first instrumented probe into Jupiter's atmosphere. In support of this navigation work, geophysical parameters of the Jovian system have been determined. These include an estimate of the third-order gravity field of Io, masses and ephemerides of Io and Europa, and a revision to the mass of Jupiter. These results are consistent with previously published results for Voyagers 1 and 2. A new Jupiter ephemeris was also computed from the tracking data. Jupiter showed a significant  $2\sigma$  shift in position with respect to the Jet Propulsion Laboratory ephemeris DE-143. Subsequently, using this updated ephemeris, accurate reconstructions of the encounters of the Galileo spacecraft pair (orbiter and probe) with Jupiter and Io were possible.**

## Introduction

THE Galileo mission is a significant development in the history of spaceflight, for Galileo is the first spacecraft to deliver a probe to, and enter into orbit around, an outer planet. Galileo's nominal mission orbiting the planet Jupiter will last for two years and is scheduled to end in December 1997. We only describe the navigation events and results occurring on approach to Jupiter, preceding the commencement of orbital activities. Because delivering the orbiter and probe to their respective targets required guidance, we describe the Jupiter-approach trajectories and provide comparisons with a priori predictions.

The first major section addresses the probe and its delivery to Jupiter, whereas the second major section details the orbiter trajectory to Io. Additionally, in support of the navigation activities we also compute new ephemerides for Jupiter, Io, and Europa, estimate a third-order gravity field for Io, and revise the mass of Jupiter. Background information describing the spacecraft and its mission to Jupiter are documented in the literature.<sup>1–4</sup>

In general, solutions computed with data to time  $t_0$  predict spacecraft states at some future time  $t_n$ . Those predictions of spacecraft paths are generated by mapping solutions at  $t_0$  out to  $t_n$  by numerical integration of the epoch state solution. On the other hand, computing the actual state achieved by the trajectory at  $t_n$  is an a posteriori calculation encompassing all data up to, and often beyond,  $t_n$ .

Spacecraft trajectory predictions are described in terms of the Bplane, a useful method for visualizing mapped dispersions. Uncertainties at the target body may be visualized in probability space as an ellipse placed perpendicular to the incoming trajectory, at the point of closest approach. This plane is the Bplane, and an illustration of its coordinate system is provided in Fig. 1. The radius from the center of the target planet to the point on the incoming asymptote intersecting the Bplane is called the impact parameter  $B$ . The elliptical area represents an uncertainty dispersion and is one measure of the statistical uncertainty in the predicted path of the spacecraft.

Significant mission events associated with critical navigation activities are discussed in sequential order and are chronicled in Table 1.

## Atmosphere Probe

### Probe Release

After an interplanetary voyage of six years, Galileo's Jupiter encounter began on April 12, 1995, with a small thrusting event that placed the spacecraft on a path toward its Jovian target. That maneuver, the 23rd trajectory correction maneuver (TCM) for Galileo (designated TCM23), was designed to send the probe (after its subsequent release from the orbiter) into Jupiter's atmosphere. The maneuver magnitude equaled  $8 \text{ cm s}^{-1}$  and targeted the probe sufficiently close to the required entry corridor that a subsequent maneuver scheduled for June (TCM24) was determined to be unnecessary and was canceled.

On July 13, the spacecraft released the atmosphere probe. (For probe release, the nominal spacecraft spin rate was increased from 2.89 to 10.5 rpm to stabilize the probe. Spin rate is changed by firing thrusters perpendicular to the spin axis; however, an imbalance in thruster pointing direction yields a net velocity change to the spacecraft during spin rate changes.) The probe target lay near the Jupiter equator at an altitude of 450 km relative to the 1-bar level of Jupiter's atmosphere. To mitigate excessive decelerations, prevent skipping off the atmosphere, and at the same time maintain radio link margins, probe targeting parameters consisted of flight-path angle with respect to the atmosphere (relative flight-path angle), entry latitude, and entry time. To satisfy probe objectives, trajectory designers insisted that the probe enter Jupiter with a relative path angle of  $-8.60 \pm 1.4$  deg (99th percentile certainty) at a latitude of  $6.57^\circ \pm 0.5^\circ$  Jupiter true equator of date (JTED), on Dec. 7, 22:04:26  $\pm$  480 s universal time coordinated (UTC) spacecraft event time (SCET). Estimates from the tracking data of selected propulsive events occurring near probe-release time are listed in Table 2.

### Probe Trajectory

The trajectory the probe followed to Jupiter was inferred from orbiter tracking data as the probe was not tracked independently. Initially, the probe state was deduced by numerical propagation of the probe from the time of separation based on a prior determination of the orbiter state. Later, after the Jupiter encounter, the probe epoch state was determined a posteriori by combining an orbiter state determination, Jupiter ephemeris estimation, and (following probe signal playback) analysis of probe-entry telemetry. (Accelerometer data from probe telemetry revealed the actual entry time.) For the reconstruction, an updated state and revised models were sufficient to yield a well-determined probe trajectory and covariance at Jupiter.

The dominant systematic errors included uncertainties in spacecraft epoch state, Jupiter's ephemeris, probe separation  $\Delta V$ , and probe spin-up  $\Delta V$ . Probe separation  $\Delta V$  was of significant concern for reconstructing the probe trajectory because the separation mechanism (a spring-loaded device) was poorly characterized. The probe spin-up  $\Delta V$  should have equaled zero, inasmuch as spin-up thruster pulsings were designed to cancel translational movements, but

Received Nov. 18, 1996; revision received April 21, 1997; accepted for publication May 2, 1997. Copyright © 1997 by the American Institute of Aeronautics and Astronautics, Inc. All rights reserved.

\*Member of the Engineering Staff, Navigation and Flight Mechanics. Member AIAA.

†Member of the Engineering Staff, Navigation and Flight Mechanics.

‡Member of the Technical Staff; retired.



assigned per-pass a priori measurement uncertainties (weights) between 0.5 and 5 mms<sup>-1</sup> (7–70 mHz), with the mode being about 2 mms<sup>-1</sup>. After JOI, a solar conjunction on Dec. 19 imposed a data blackout from Dec. 10–28 (–7 to +7 deg sun–Earth–orbiter angle), when tracking data were not received from the spacecraft. For approximately three or four days on each side of the conjunction gap, significantly larger residuals were evident, with a postfit data noise in the Doppler residuals of 3.7-mms<sup>-1</sup> rms. Except for these passes straddling conjunction, however, data quality was satisfactory, exhibiting Doppler residual noise of 0.7-mms<sup>-1</sup> rms.

From late October to mid-November, three optical navigation images were scheduled to supplement the baseline radiometric two-way Doppler data. Optical navigation data consist of cross line-of-sight measurements of the positions of, in this case, Io and Europa, as viewed from the spacecraft. A tape recorder anomaly on Oct. 11, however, ultimately resulted in the loss of these images, thereby eliminating this powerful target-relative data type.

One-way Doppler tracking around the Io encounter admitted an immediate reconstruction of the flyby conditions. (Two-way Doppler was unavailable from Dec. 7, 4:16 UTC, through Dec. 8, 7:24, because of preparations for probe relay and orbit insertion.) Accuracy of one-way data is a function of the frequency stability of the onboard ultrastable oscillator (USO) and is significantly less than that of two-way data. Nevertheless, one-way Doppler may be characterized adequately for navigation purposes by estimating a one-way Doppler bias, drift, and drift rate (using adjacent two-way Doppler as a reference). At the time of the Io encounter, the USO showed a bias relative to the two-way carrier of

–36.6 ± 1.0 Hz (a hundredfold increase in the one-way Doppler uncertainty with respect to the bias uncertainty of the previous day), a drift of –0.49 ± 0.26 mHzs<sup>-1</sup> (consistent with previous estimates), and a negligible drift rate of –2.4 ± 16.8 nHzs<sup>-2</sup>. Shortly after the encounter (Dec. 7, 19:42), we observed significant degradation in the quality of the one-way data severe enough such that all one-way data after that time were removed from the fit. Electron fluence, originating in the Jovian radiation environment and Io torus, is believed to be the source of this degradation, as well as the hundredfold increase in measurement uncertainty at the time of closest approach. The one-way data before this time were assigned per-pass a priori weights between 3 and 9 mms<sup>-1</sup> (20–60 mHz). For comparison, postfit rms one-way residuals showed a scatter of 2–6 mms<sup>-1</sup>, indicating the data were of significant value to the solution.

The tape recorder anomaly of Oct. 11 forced the cancellation of imaging science at Io (in addition to the optical navigation cancellations), which led in turn to relaxed targeting requirements. Without science imaging of Io, camera pointing accuracies were not important; instead, spacecraft energy change for orbit insertion became the sole driver of the delivery. Because the encounter was to occur at equatorial latitudes, spacecraft altitude would correlate with the *B · T* component of Io’s Bplane. The energy change imparted to the spacecraft, a function of altitude, would therefore also correlate with *B · T*. The *B · R* component was less important due to focusing effects and, therefore, latitude errors were not significant for an orbit energy change (to first order).

Estimated quantities consisted of orbiter state, satellite ephemerides, satellite masses (as well as the third-order gravity field of Io), Jupiter’s mass and *J*<sub>2</sub> and *J*<sub>4</sub> harmonic terms, spacecraft propulsive events, solar pressure, two-way Doppler biases, and one-way Doppler bias, drift, and drift-rate terms. A list of all modeled and estimated parameters used in the Io reconstruction is provided in Ref. 6.

Systematic errors included sources similar to the list enumerated for the probe. Other sources included additional maneuvers in the data arc, satellite ephemerides, and data biases. As contributors to the error budget, these sources were estimated in the solution.

By way of comparison with Table 4, Table 5 lists the results of the actual Jupiter/Io approach. It can be seen that degradations accompany the loss of optical data. Surprisingly, in the last week of the approach, the flight data (without optical aid) produced smaller

**Table 4** A priori predicted Io Bplane orbit determination uncertainties, 1σ

Data cutoff time (days before Io)	TCM supported	<i>B · R</i> , km	<i>B · T</i> , km	LTOF, <sup>a</sup> s	Number of navigation images
–114	26	258	395	28.4	0
–27	27	64	108	8.1	1
–19	28	60	110	8.3	1
–6	28 A	32	54	4.1	3
–3	29 (JOI)	32	26	1.4	3

<sup>a</sup>Linearized time of flight.

**Table 5** Io Bplane history, 1σ Earth mean orbit of 1950 (no optical navigation images)

Data cutoff time (days from Io)	TCM supported	<i>B · R</i> , km	<i>B · T</i> , km	TCA, <sup>a</sup> 12/7/95 UTC	Altitude, km
Target	—	87	2847	17:45:44	1000
–114	26	433 ± 373	925 ± 437	41:55 ± 29	–800 ± 429
–27	27	205 ± 120	2925 ± 131	45:39 ± 11	1084 ± 126
–19	28	226 ± 102	2919 ± 149	45:40 ± 12	1080 ± 145
–6	28 A	420 ± 70	2753 ± 34	45:53 ± 2.1	937 ± 36
–3	29 (JOI)	392 ± 71	2708 ± 23	45:57 ± 0.8	888 ± 27
+0.01	—	474 ± 2	2699 ± 2	45:58 ± 0.1	892 ± 2
+55	—	466.4 ± 0.3	2705.6 ± 0.2	45:58 ± 0.0	897.3 ± 0.2

<sup>a</sup>Time of closest approach.

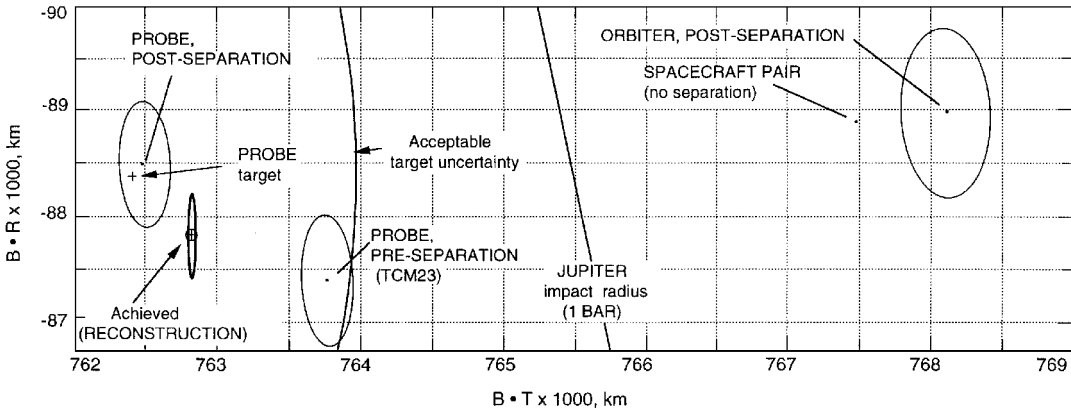


**Fig. 2** Probe delivery, Jupiter Bplane, Earth mean orbit of 1950 at Dec. 5, 1995, 22:00 UTC (1σ).

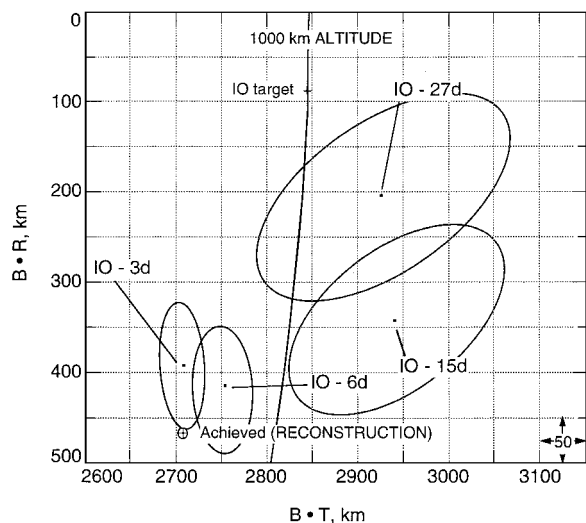


Fig. 3 Orbiter delivery, Io Bplane, Earth mean orbit of 1950 ( $1\sigma$ ).

uncertainties in  $B \cdot T$  than were predicted from the simulation (with optical data). This difference is explainable in terms of moderately dissimilar estimation strategies, data weighting schemes, and tracking coverage assumptions. The  $B \cdot R$  uncertainty remained large due to the lack of optical data. (In general,  $B \cdot R$  knowledge will improve marginally with additional Doppler but improves substantially with the optical component.)

The movement of the spacecraft in the Bplane in the month preceding the encounter is shown in Table 5 and in Fig. 3. Note that the altitude remained within approximately  $\pm 150$  km of the 1000-km target altitude at all times, although the latitude deviated from the target by as much as  $8^\circ$ .

Because of arrival options at Ganymede in June 1996, the low altitude predicted by the TCM28A and TCM29 deliveries had surprisingly benign consequences on the trajectory (assuming a nominal JOI). The additional  $\Delta V$  imparted to the orbiter by the low flyby was found to (serendipitously) advance the arrival date at Ganymede by nearly one Ganymede orbital period (one week). Thus, the orbiter could remain on its low trajectory (thereby eliminating last-minute trajectory changes), perform the nominal JOI burn (thereby eliminating last-minute main-engine parameter changes), reach Ganymede with a nearly nominal sequence of events, and still remain within the orbiter's budgeted propellant allotment.

The orbiter's encounter with Io provided an unprecedented opportunity to directly measure the location of Io relative to Earth. (The Io-spacecraft measurement was 540 times more sensitive than the one provided by Voyager.) By simultaneously estimating the Jupiter-spacecraft state, Io's location with respect to Jupiter was accurately inferred. This measurement was obtained by radiometric means during the flyby and indicated an error in Io's Jovicentric state at the time of the flyby of 9 km and  $2 \text{ ms}^{-1}$  rss, with respect to the extant Jet Propulsion Laboratory a priori satellite ephemeris JUP076.

Relative to JUP076, the greatest difference was found along the out-of-plane component. That difference oscillated over one orbital period from approximately  $-50$  to  $+50$  km, a little more than  $1\sigma$  a priori. This was expected, as that direction represents the greatest uncertainty in the Io ephemeris. Furthermore, the downtrack difference varied between 0 and 20 km, implying an approximate downtrack secular bias of about 10 km in JUP076. That bias may indicate a mean motion error in Io's ephemeris. A definitive statement must await further data. Radial differences oscillated between  $-5$  and 5 km. The latter differences are small, about  $1\sigma$ . (For comparison, Ref. 6 lists JUP076 a priori state uncertainties.)

Similarly, new insights were forthcoming at Europa, as that flyby provided data 40 times more sensitive than Voyager. (Galileo's altitude at the time of closest approach to Europa was 32,994 km.) A satellite state measurement equivalent to that for Io was obtained for Europa, and an adjustment in its Jovicentric state at the time of the flyby was computed: 108 km and  $3 \text{ ms}^{-1}$  rss. Downtrack error dominated this determination, showing a consistent 40 km bias (about  $1\sigma$  offset) modulated with a periodic difference, or uncer-

Table 6 Io gravity

<i>A priori characteristics</i>	
Data arc	11/12–1/31
70 days arc length	
Uncorrelated $J_2$ , $C_{22}$ , and $S_{22}$	
A priori $J_2 \times 10^{-6}$	$2000 \pm 610$
A priori $C_{22} \times 10^{-6}$	$600 \pm 70$
<i>Results</i>	
Flyby altitude	$897.3 \pm 0.2$ km
TCA <sup>a</sup> (UTC)	$45 \text{ min } 58 \text{ s} \pm 0.01 \text{ s}$
$J_2 \times 10^{-6}$	$1863 \pm 423$
$C_{22} \times 10^{-6}$	$547 \pm 14$
$S_{22} \times 10^{-6}$	$19 \pm 12$
$GM_{\text{Io}}$	$5960 \pm 3 \text{ km}^3 \text{ s}^{-2}$
Io adjustment	$9$ km

<sup>a</sup>Time of closest approach.

tainty, between the ephemerides of about the same magnitude. (This downtrack bias also suggests a mean motion error in JUP076.) Out-of-plane periodic differences are significantly larger ( $\approx 200$  km), but the mean of this component is unbiased. These out-of-plane (and radial) differences oscillating around zero suggest small adjustments to the node or inclination have occurred.

The Io encounter acquired the first ever sampling of Io's gravity field, for which the following parameters were estimated: mass and a third-order gravity field (but we report only the significant second-order coefficients). The data near closest approach exhibited a uniform scatter with white rms noise of  $2.4 \text{ mms}^{-1}$ , indicating the estimated model fit well with the data. The details of this gravity determination are outlined in Table 6. Masses are expressed as the product  $GM$ , that is, the universal gravitational constant  $G$  times the mass of the body in kilograms  $M$ , in units of ( $\text{km}^3 \text{ s}^{-2}$ ). The mass error estimates presented here represent our evaluation of real, as opposed to formal,  $1\sigma$  errors.

Pending additional data, we estimate the following values for Io's gravity field:  $GM_{\text{Io}} = 5960 \pm 3 \text{ km}^3 \text{ s}^{-2}$  (within  $1\sigma$  of the Voyager results),  $J_2 = 1863 \pm 423 \times 10^{-6}$ ,  $C_{22} = 547 \pm 14 \times 10^{-6}$ , and  $S_{22} = 19 \pm 12 \times 10^{-6}$ . Although these results are still preliminary, it can be shown that the estimates suggest a differentiated structure for Io.<sup>7</sup> That is, Io can be shown to contain an iron or iron-sulphide core with a radius of approximately 50% the satellite radius.

A preliminary gravity map of Io is reproduced in Fig. 4a, which assumes a synchronously rotating satellite in tidal and rotational equilibrium. In general, a gravity map spatially displays potential fields and indicates mass inhomogeneities. Contour lines map the magnitude of the local gravity acceleration measured in mGal ( $0.01 \text{ mms}^{-2}$ ). Solid lines represent positive accelerations (with respect to an equipotential surface), whereas dashed lines represent negative values. Note that the tidal distortion bulge ( $C_{22}$ ) is clearly indicated by gravity mounds at the sub-Jupiter point ( $0^\circ$  longitude) and at the anti-sub-Jupiter point ( $180^\circ$ ). The spacecraft's closest approach occurred over a point at  $-10^\circ$  latitude,  $-100^\circ$  longitude. Figure 4b indicates the  $1\sigma$  uncertainty associated with the measurements in Fig. 4a.

For the mass of Europa, we compute  $GM_{\text{Eur}} = 3199 \pm 5 \text{ km}^3 \text{ s}^{-2}$ , a value within the measurement uncertainty of Voyagers 1 and 2.

Our best estimate to date of the Jupiter ephemeris indicates a shift of greater than  $2\sigma$  in Jupiter's position from the latest pre-Galileo Jet Propulsion Laboratory planetary ephemeris, DE-143. These corrections are listed in Table 7. The precision of this measurement has improved significantly from previous determinations by the Pioneer, Voyager, and Ulysses spacecraft. Radial uncertainty decreases by a factor of five and downtrack uncertainty improves sevenfold, with respect to DE-143 (Ref. 6). Jupiter's out-of-plane (normal) uncertainty decreases by a factor of four.

Revised estimates for Jupiter's mass and its second and fourth zonal harmonic coefficients, i.e.,  $GM_{\text{Jup}}$ ,  $J_2$ , and  $J_4$ , are also listed here.  $GM_{\text{Jup}}$  was estimated to equal  $126,712,718 \pm 85 \text{ km}^3 \text{ s}^{-2}$ , a value within the uncertainty quoted by Campbell and Synnott.<sup>8</sup> The tabulated values of  $J_2$  and  $J_4$  do not differ from values in the literature, although we have improved the precision of the estimate. Our updated values and uncertainties are listed in Table 8. (The

ephemeris and gravity estimates were determined with tracking data acquired after the Jupiter encounter and are refinements of previous ephemerides determined prior to and during the Io/Jupiter encounter.)

JOI Burn

The JOI burn model consisted of the following parameters: JOI start time, burn duration, burn direction (right ascension  $\alpha$ , declination  $\delta$ ), and thrust (modeled with a fifth-degree polynomial).

**Table 7** Jupiter’s position corrections (with respect to DE-143) and formal  $1\sigma$  uncertainty, sun-centered, Earth mean orbit of 1950, Jupiter orbit fixed, Dec. 7, 1995, 17:46 UTC SCET

Radial, km	Downtrack, km	Normal, km
$18.8 \pm 2.0$	$-69.3 \pm 4.9$	$549.4 \pm 58.8$

The nominal thrust profile of JOI is illustrated in Fig. 5. Because a fifth-degree polynomial cannot, in general, adequately fit a curve of the shape illustrated in Fig. 5, an exponentially decaying acceleration of 5-min duration was independently estimated during the first 5 min of JOI to supplement the JOI thrust model during that time. Additionally, the spin-up and spin-down activities occurring on either side of JOI were modeled with impulsive burns (instantaneous  $\Delta V$  components along three orthogonal axes).

Table 9 lists the reconstructed values and uncertainties of JOI, as well as their offsets from the nominal values. We determined an overburn of 0.1% for JOI  $\Delta V$  and a spacecraft pointing error of 1 mrad.

**Table 8** Jupiter gravity

$GM_{\text{Jup}}, \text{ km}^3 \text{ s}^{-2}$	$J_2, \times 10^{-6}$	$J_4, \times 10^{-6}$
$126,712,718 \pm 85$	$14,736 \pm 0.5$	$-587 \pm 2.5$

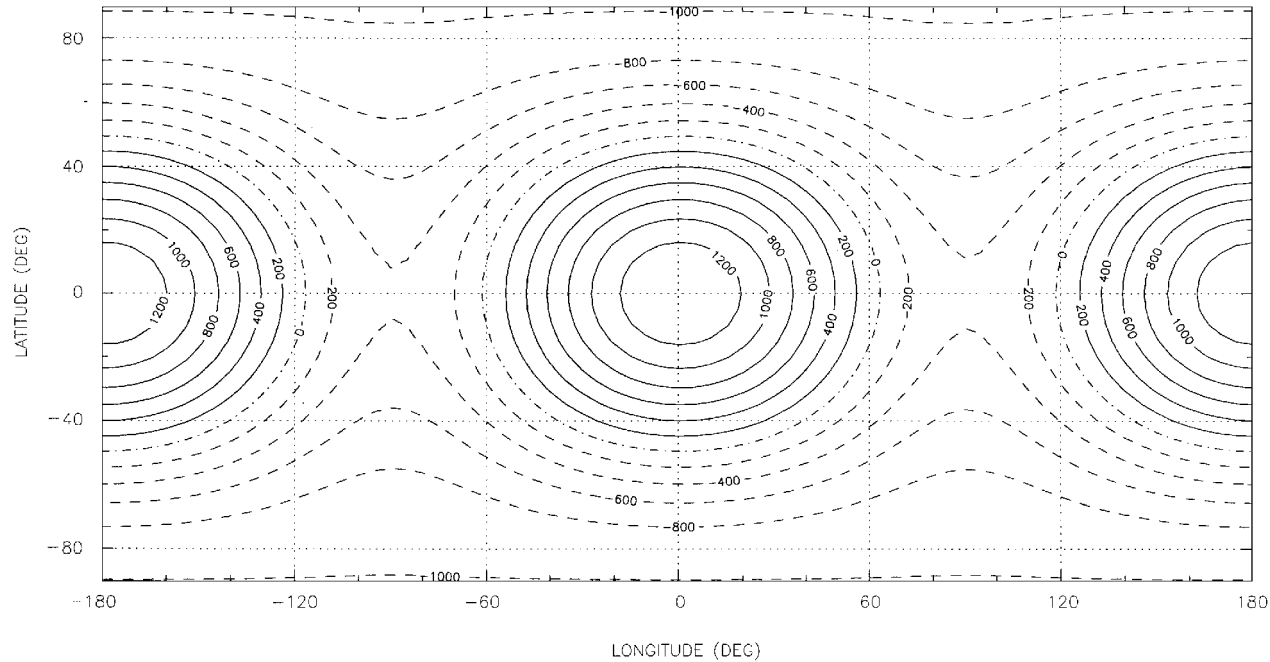


**Fig. 4a** Io  $3 \times 3$  gravity field (mGal); closest approach point at latitude  $-10^\circ$ , longitude  $-100^\circ$ .

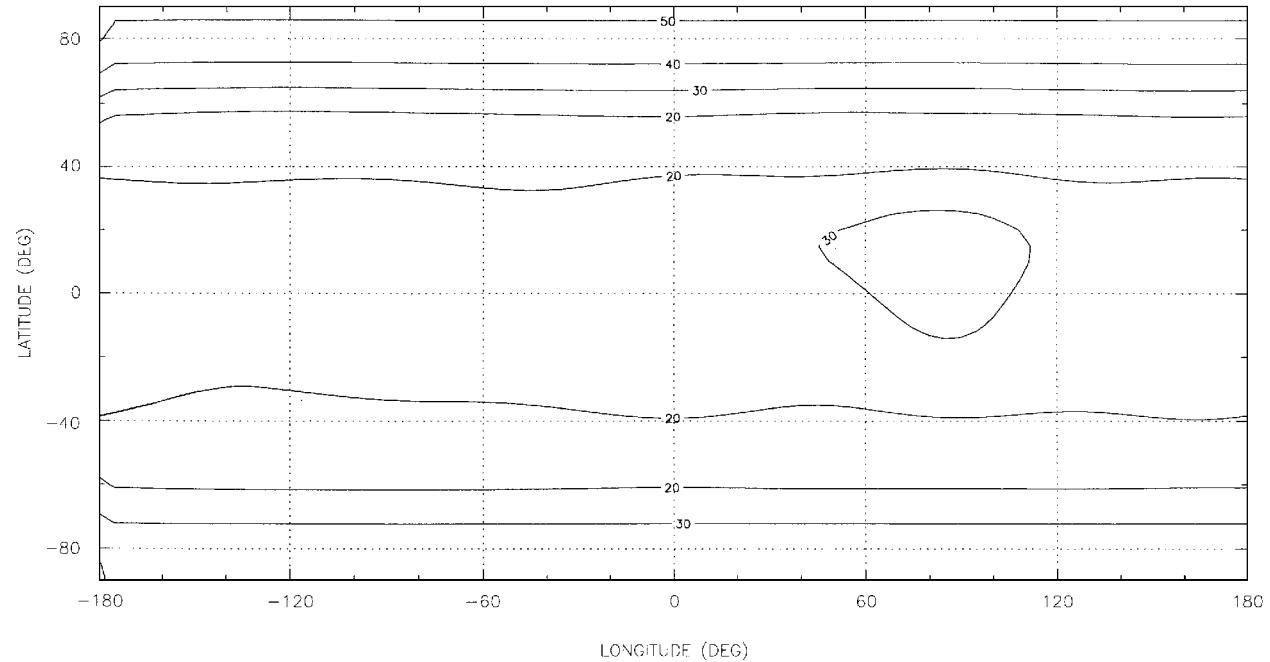


**Fig. 4b** Io  $3 \times 3$  gravity field  $1\sigma$  uncertainty (mGal).

Table 9 JOI events, 1σ

Events	A priori	Reconstruction	Deviation from a priori, σ <sup>a</sup>
Spin up for JOI, cms <sup>-1</sup>	—	6.64 ± 2.37	—
JOI			
ΔV, ms <sup>-1</sup>	644.400	645.301 ± 0.552	<1 (+0.14%)
α, deg	87.700	87.765 ± 0.0063	2.8
δ, deg	27.600	27.609 ± 0.024	<1
Start time, UTC	00:27:24.5	00:27:22.0 ± 0.2 s	2.5 (−2.5 s)
Duration	48 min 37.1 s	49 min 4.4 s ± 0.3 s	5 (+27.3 s)
Average thrust, N	391.44	386.00 ± 0.33	<1 (−1.4%)
Spin down from JOI, cms <sup>-1</sup>	—	2.93 ± 2.06	—

<sup>a</sup>The deviation from a priori is with respect to orbiter capability, not with respect to required JOI accuracy. These deviations are well within the 1σ error bars of JOI requirements.

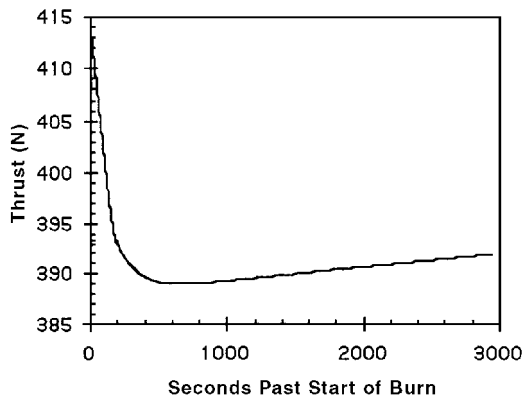


Fig. 5 JOI thrust profile.

Closing Remarks

Deliveries of the Galileo atmosphere probe and orbiter to Jupiter and Io, respectively, met their objectives and were highly successful events. The probe fell well within acceptable limits, missing its target by approximately 0.3σ. The orbiter missed the Io target by 3σ (relative to the last trajectory correction opportunity), but this undershoot was known in advance and was supported and approved by the Galileo project (the loss of optical navigation data contributed significantly to this error). The effect on the mission was benign. Probe entry occurred on Dec. 7, 1995, 22:04:43.9 UTC SCET ± 3.1 s. The spacecraft’s closest approach to Io occurred on Dec. 7, 1995, 17:45:58.4 UTC SCET ± 0.004 s, at a distance of 897.3 ± 0.2 km and latitude of −9.55° ± 0.01°. An Io gravity field and new Io ephemeris were computed as an integral part of the spacecraft’s encounter reconstruction. Encounter data also determined a 2σ shift in the position of Jupiter.

Acknowledgment

The work described in this paper was performed at the Jet Propulsion Laboratory, California Institute of Technology, under a contract with NASA.

References

<sup>1</sup>D’Amario, L. A., Byrnes, D. V., Haw, R. J., Kirhofer, W. E., Nicholson, F. T., and Wilson, M. G., “Navigation Strategy for the Galileo Jupiter Encounter and Orbital Tour,” *Astrodynamics 1995: Proceedings of the AAS/AIAA Astrodynamics Specialist Conference*, Univelt, San Diego, CA, 1996, pp. 1387–1411.

<sup>2</sup>Antreasian, P. G., Nicholson, F. T., Kallemeyn, P. H., Bhaskaran, S., Haw, R. J., and Halamek, P., “Galileo Orbit Determination for the Ida Encounter,” *Advances in the Astronautical Sciences 1994*, Vol. 87, Pt. 2, Univelt, San Diego, CA, 1994, pp. 1027–1048.

<sup>3</sup>O’Neil, W. J., Ausman, N. E., Landano, M. R., Mitchell, R. T., and Reichert, R. J., “Galileo Preparing for Jupiter Arrival,” 45th Congress of the International Astronautical Federation, Paper IAF-94.Q.5.355, Jerusalem, Israel, Oct. 1994.

<sup>4</sup>Miller, L. J., Miller, J. K., and Kirhofer, W. E., “Navigation of the Galileo Mission,” AIAA Paper 83-0102, Jan. 1983.

<sup>5</sup>Hintz, G. R., and Longuski, J. M., “Error Analysis for the Delivery of a Spinning Probe to Jupiter,” *Journal of Guidance, Control, and Dynamics*, Vol. 8, No. 3, 1985, pp. 384–390.

<sup>6</sup>Haw, R. J., Antreasian, P. G., Graat, E. J., McElrath, T. P., and Nicholson, F. T., “Galileo at Jupiter: Delivery Accuracy,” *Astrodynamics 1996: Proceedings of the AAS/AIAA Astrodynamics Specialist Conference*, Univelt, San Diego, CA, 1996, pp. 385–397.

<sup>7</sup>Anderson, J. D., Sjogren, W. L., and Schubert, G., “Galileo Gravity Results and the Internal Structure of Io,” *Science*, Vol. 272, No. 5262, 1996, pp. 709–712.

<sup>8</sup>Campbell, J. K., and Synnott, S. P., “Gravity Field of the Jovian System from Pioneer and Voyager Tracking Data,” *Astronomical Journal*, Vol. 90, No. 2, 1985, pp. 364–372.

F. H. Lutze Jr.  
Associate Editor